TSINGHUA SCIENCE AND TECHNOLOGY
ISSN 1007-0214 06/18 pp269-275
Volume 12, Number 3, June 2007

# Optimal Kinematic Design of a 2-DOF Planar Parallel Manipulator*

WU Jun (吴 军), LI Tiemin (李铁民)**, LIU Xinjun (刘辛军), WANG Liping (王立平)

**Institute of Manufacturing Engineering, Department of Precision Instruments and Mechanology, Tsinghua University, Beijing 100084, China**

**Abstract:** Closed-form solutions were developed to optimize kinematics design of a 2-degree-of-freedom (2-DOF) planar parallel manipulator. The optimum design based on the workspace was presented. Meanwhile, a global, comprehensive conditioning index was introduced to evaluate the kinematic designs. The optimal parallel manipulator is incorporated into a 5-DOF hybrid machine tool which includes a 2-DOF rotational milling head and a long movement worktable. The results show that the planar parallel manipulator-based machine tool can be successfully used to machine blades and guide vanes for a hydraulic turbine.

**Key words:** planar parallel manipulator; global conditioning index; hybrid machine tool

## Introduction

Parallel mechanisms are capable of very fast and accurate motion, possess higher average stiffness characteristics throughout their workspace, have lower inertia, and can manipulate heavier payloads than their serial counterparts. Therefore, parallel mechanisms have been studied extensively by numerous researchers in manufacturing, primarily as platforms for computer numerical control machining. The Gough-Stewart platform was the most popular parallel kinematic machine configuration when parallel kinematic machine were first developed. Applications within the robotics community range from high-speed manipulation[1] to force-torque sensing[2]. But the Gough-Stewart platform has some disadvantages for manufacturing applications such as its relatively small useful workspace, complex direct kinematics, and design difficulties.

Parallel manipulators with less than 6 DOFs are relatively easy to design and their kinematics can be described in closed form. Therefore, parallel manipulators with less than 6 DOFs, especially 2 or 3 DOFs, have increasingly attracted attention[3-5]. Parallel manipulators with 2 or 3 translational DOFs play important roles in industry and can be applied in parallel kinematics machines[6], pick and place applications[7], and other fields. Most existing 2-DOF planar parallel manipulators are the well-known five-bar mechanism with prismatic actuators or revolute actuators[8,9]. The manipulator output is the translational motion of a point on the end-effector and the end-effector orientation cannot remain constant.

The kinematic design methodology is one of the key parts of kinematic design theory for parallel mechanisms. The optimum design can be based on various evaluation criteria involving stiffness[10], dexterity, or a global conditioning index[11,12]. Hence, there has not been one widely accepted design method. Huang et al.[13] presented a hybrid method based on a conditioning index, while Liu et al.[14] gave a global stiffness

Received: 2006-06-02; revised: 2006-08-21

* Supported by the National Natural Science Foundation of China (No. 50305016) and the National High-Tech Research and Development (863) Program of China (Nos. 2004AA424120 and 2005AA424223)

** To whom correspondence should be addressed.
E-mail: litm@mail.tsinghua.edu.cn; Tel: 86-10-62792792

index similar to the global conditioning index.

This paper describes the analysis of a planar parallel manipulator with two translational DOFs which differs from the conventional five-bar mechanism in that a parallelogram structure is used in each chain. The kinematics are analyzed to get an optimum kinematic design by minimizing a global, comprehensive conditioning index. The results give the optimal link lengths.

A 5-DOF hybrid machine tool was developed with a serial-parallel architecture with a parallel manipulator combined with a 1-DOF translational worktable and a 2-DOF rotational milling head. The hybrid machine tool using the planar parallel manipulator has been used to mill the blades and guide vanes of a hydraulic turbine to show that the hybrid machine tool is suitable for the manufacturing industry

# 1 Structure Description

The 2-DOF parallel manipulator is shown in Fig. 1. The mechanism is composed of a gantry frame, a moving platform, two active sliders, and two kinematic chains. Each chain is built as a parallelogram. As designed, the manipulator is over-constrained since one parallelogram link and another single link are enough for the moving platform to posses 2 translational DOFs. Two parallelogram chains were used to increase the stiffness and make the structure symmetric.

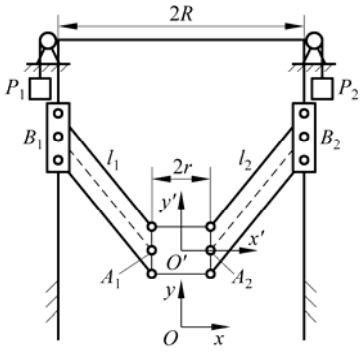


**Fig. 1 Kinematic model**

Counterweights $P_1$ and $P_2$ (see Fig. 1) were added to the mechanism to improve the load capacity and acceleration of the actuator. The sliders are driven independently by two servo motors on the columns to slide along the guide ways mounted on the columns, thus moving platform with a 2-DOF purely translational motion in a plane.

# 2 Kinematics and Singularities

## 2.1 Inverse kinematics

Since the motions of two links of each kinematic chain are identical due to the parallelogram structure, the chain model can be simplified as a link $A_iB_i$ ($i=1,2$) as illustrated in Fig. 1. The base coordinate system $O$-$xy$ is attached to the base with its $y$ axis vertical through the midpoint of $\overline{B_1B_2}$. A moving coordinate system $O'$-$x'y'$ is fixed on the moving platform. $\boldsymbol{r}_{A_i}$ and $\boldsymbol{r}_{B_i}$ are the position vectors of the joint positions $A_i$ and $B_i$, respectively. $2r$ is the moving platform width and $2R$ is the width between the two columns.

The position vector of the origin $O'$ with respect to the coordinate system $O$-$xy$ is defined as

$$\boldsymbol{r}_{O'}=\begin{bmatrix}x & y\end{bmatrix}^{\mathrm{T}} \tag{1}$$

The position vector of joint position $A_i$ in $O'$-$x'y'$ is

$$\boldsymbol{r}'_{A_1}=\begin{bmatrix}-r & 0\end{bmatrix}^{\mathrm{T}} \tag{2}$$

$$\boldsymbol{r}'_{A_2}=\begin{bmatrix}r & 0\end{bmatrix}^{\mathrm{T}} \tag{3}$$

Then the position vector of $A_i$ in the base coordinate system $O$-$xy$ can be expressed as

$$\boldsymbol{r}_{A_i}=\boldsymbol{r}_{O'}+\boldsymbol{r}'_{A_i} \tag{4}$$

The position vector of each joint position $B_i$ in $O$-$xy$ is

$$\boldsymbol{r}_{B_1}=\begin{bmatrix}-R & y_1\end{bmatrix}^{\mathrm{T}} \tag{5}$$

$$\boldsymbol{r}_{B_2}=\begin{bmatrix}R & y_2\end{bmatrix}^{\mathrm{T}} \tag{6}$$

Thus, the constraint equation associated with the $i$-th kinematic chain can be written as

$$\boldsymbol{r}_{A_i}-\boldsymbol{r}_{B_i}=l_i\boldsymbol{n}_i,\quad i=1,2 \tag{7}$$

where $l_i$ and $\boldsymbol{n}_i$ denote the length and the unit vector of the $i$-th link, respectively.

Taking the 2-norm of both sides of Eq. (7) gives

$$y_1=y\pm\sqrt{l_1^2-\left(x-r+R\right)^2} \tag{8}$$

$$y_2=y\pm\sqrt{l_2^2-\left(x+r-R\right)^2} \tag{9}$$

For the configuration shown in Fig. 1, the inverse solutions of the kinematics are

$$y_1=y+\sqrt{l_1^2-\left(x-r+R\right)^2} \tag{10}$$

$$y_2 = y + \sqrt{l_2^2 - (x + r - R)^2} \tag{11}$$

From Eqs. (10) and (11), the solutions for the direct kinematics of the manipulator can be expressed as

$$y = \frac{-(2af - 2y_1) \pm \sqrt{f^2 + 4(a^2+1)(l_1^2 - y_1^2 - f^2)}}{2(a^2+1)} \tag{12}$$

where

$$a = \frac{y_1 - y_2}{2(R-r)}, \quad b = \frac{y_2^2 - y_1^2}{4(R-r)}, \quad c = \frac{l_1^2 - l_2^2}{4(R-r)},$$
$$f = R - r + b + c, \quad x = ay + b + c \tag{13}$$

For the configuration as shown in Fig. 1, the "±" of Eq. (12) should be only "—".

Equations (7)-(13) show that the direct and inverse kinematics of the manipulator can be described in closed form.

### 2.2 Singularity analysis

Taking the derivatives of Eq. (10) and Eq. (11) with respect to time gives

$$\dot{y}_1 = \dot{y} - \frac{x - r + R}{\sqrt{l_1^2 - (x - r + R)^2}} \dot{x} \tag{14}$$

$$\dot{y}_2 = \dot{y} - \frac{x + r - R}{\sqrt{l_2^2 - (x + r - R)^2}} \dot{x} \tag{15}$$

Equations (14) and (15) can be rearranged in matrix form as

$$\begin{bmatrix} \dot{y}_1 \\ \dot{y}_2 \end{bmatrix} = \boldsymbol{J} \begin{bmatrix} \dot{x} \\ \dot{y} \end{bmatrix} \tag{16}$$

where $\boldsymbol{J}$ is the Jacobian expressed as

$$\boldsymbol{J} = \begin{bmatrix} -\dfrac{x - r + R}{\sqrt{l_1^2 - (x - r + R)^2}} & 1 \\ -\dfrac{x + r - R}{\sqrt{l_2^2 - (x + r - R)^2}} & 1 \end{bmatrix} \tag{17}$$

Because singularities lead to a loss of controllability and degradation of the natural stiffness of the manipulators, they must be avoided in the task workspace. Singularities can be classified as direct kinematic singularities, inverse kinematic singularities, and combined singularities[15], and can be distinguished by the manipulator Jacobian. When one of the links is horizontal, the manipulator experiences an inverse kinematic singularity.

Direct kinematic singularities occur when one link of a chain and a link of the other chain are collinear. Since $l_1 + l_2 > 2R$, combined singularities cannot occur in this manipulator. Figure 2 shows one example of each kind of singularity. In practical applications, singularities are avoided by limiting the task workspace.

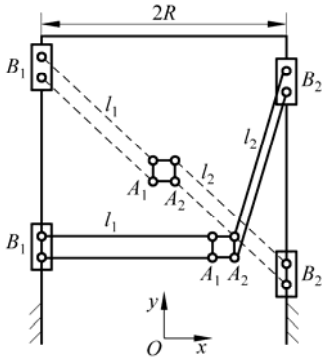


**Fig. 2 Singular configurations**

## 3 Workspace Analysis

The workspace for the 2-DOF planar parallel manipulator is a region of the plane derived by the workspace of the reference point $O'$ of the moving platform. Equations (10) and (11) can be rewritten as

$$(x - r + R)^2 + (y - y_1)^2 = l_1^2 \tag{18}$$

$$(x + r - R)^2 + (y - y_2)^2 = l_2^2 \tag{19}$$

Therefore, the reachable workspace of the reference point $O'$ is the intersection of the sub-workspaces associated with the two kinematic chains as shown in Fig. 3.

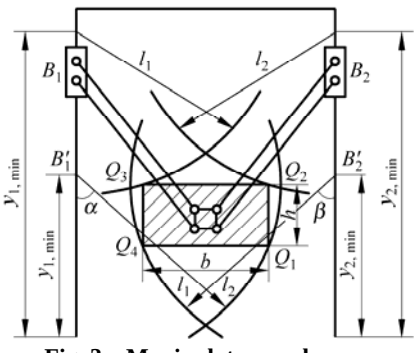


**Fig. 3 Manipulator workspace**

The task workspace is a part of the reachable workspace. In practical applications, the task workspace is usually defined as a rectangular area in the reachable workspace.

Let the maximum limit of the angles $\alpha$ and $\beta$, which are the angles between link $A_iB_i$ ($i=1,2$) and the vertical axis, be denoted by $\alpha_{\max}$ and $\beta_{\max}$. Let $y_{i,\max}$ and $y_{i,\min}$ represent the maximum and minimum positions of the *i*-th slider. $O'$ reaches point $Q_1$ when slider $B_1$ reaches its lower limit and the value of $\alpha$ is the maximum, namely $y_1 = y_{1,\min}$ and $\alpha = \alpha_{\max}$. Similarly, $O'$ reaches point $Q_4$ when $y_2 = y_{2,\min}$ and $\beta = \beta_{\max}$.

A vertical line through $Q_1$ intersects with the upper bound of the reachable workspace at point $Q_2$. $Q_3$ is directly above $Q_4$ (see Fig. 3). The region $Q_1Q_2Q_3Q_4$ then makes up the task workspace, as a rectangle of width $b$ and height $h$, denoted by $W_t$.

# 4 Optimal Kinematic Design

## 4.1 Optimal design based on the workspace

The objective of this section is to determine the manipulator parameters for a desired workspace. The scope of optimal design can be stated as: given *r*, *b*, and *h* of $W_t$, determine *R*, $l_1$, $l_2$, and the total journey $|y_{i,\max} - y_{i,\min}|$ of the slider.

From Eqs. (10), (11), and (17), the manipulator performance is related to $R-r$ but not to $r$ or $R$ alone. Practically, $r$ should be as small as possible since smaller values of $r$ lead to smaller manipulator volumes. Usually, $r$ depends on the shaft, bearing, and tool dimensions on the moving platform. Therefore, $r$ should be given by the designer.

When the moving platform reaches the lower limit, as shown in Fig. 4, the following parametric relationships can be obtained

$$\sin\alpha_{\max} = \frac{d+b-r}{l_1} \tag{20}$$

$$\sin\beta_{\min} = \frac{d-r}{l_2} \tag{21}$$

where $d$ is the distance from the left column to the left limit of the task workspace.

In practical applications, $l_1$ should equal $l_2$ to improve the system performance and stiffness. Therefore

$$d = \frac{\sin\alpha_{\max} r + \sin\beta_{\min}(b-r)}{\sin\alpha_{\max} - \sin\beta_{\min}} \tag{22}$$

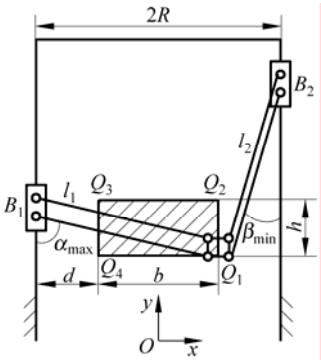


**Fig. 4 Optimal design of the manipulator**

Thus,

$$R = \frac{b}{2} + d \tag{23}$$

For $l_1 = l_2$, when the moving platform moves from point $Q_1$ to $Q_4$ along the $x$ axis, the sliding distance of the slider in the guide way should be

$$y_{B_1} = \sqrt{l_1^2 - \left(R + \frac{d}{2} - r\right)^2} - \sqrt{l_1^2 - \left(R - \frac{d}{2} - r\right)^2} \tag{24}$$

When the moving platform travels from point $Q_4$ to $Q_3$ along the $y$ direction, the sliding distance of the slider is

$$y_{B_2} = h \tag{25}$$

Hence, the total journey $|y_{i,\max} - y_{i,\min}|$ of the slider is

$$|y_{i,\max} - y_{i,\min}| = y_{B_1} + y_{B_2} \tag{26}$$

Because the optimum design based on the task workspace does not consider the dexterity and stiffness of the manipulator, the link lengths are not optimal. The optimal lengths of the links and $|y_{i,\max} - y_{i,\min}|$ for the slider are determined in the next subsection.

## 4.2 Global, comprehensive index

The condition number of the Jacobian is used as the local performance index for evaluating the velocity, accuracy, and rigidity mapping characteristics between the joint variables and the moving platform. The condition number $\kappa$ is defined as

$$1 \leqslant \kappa = \frac{\sigma_2}{\sigma_1} \leqslant \infty \tag{27}$$

where $\sigma_1$ and $\sigma_2$ are the minimum and maximum singular values of the Jacobian associated with a given

posture. $\sigma_1$ and $\sigma_2$ can be determined by solving the characteristic equation

$$\det\left(\sigma^2 \boldsymbol{I} - \boldsymbol{J}^{\mathrm{T}}\boldsymbol{J}\right) = 0 \tag{28}$$

where $\boldsymbol{I}$ denotes a unit matrix of order 2. For the parallel manipulator studied here,

$$\kappa = \sqrt{\frac{2 + s^2 + t^2 + \sqrt{(s^2 + t^2)^2 + 8st + 4}}{2 + s^2 + t^2 - \sqrt{(s^2 + t^2)^2 + 8st + 4}}} \tag{29}$$

where $s = \dfrac{x - r + R}{y - y_1}$ and $t = \dfrac{x + r - R}{y - y_2}$.

Since $\kappa$ varies with the mechanism configuration, a global performance index is used as the performance measure in the optimal kinematic design,

$$\bar{\eta} = \int_{W_{\mathrm{t}}} \kappa \mathrm{d}W_{\mathrm{t}} \Big/ \int_{W_{\mathrm{t}}} \mathrm{d}W_{\mathrm{t}} \tag{30}$$

Note that $\bar{\eta}$ itself cannot give a full description of the overall global kinematic performance due to its inability to describe the difference between the maximum and minimum values of $\kappa$. Huang et al.[7] proposed a global, comprehensive condition index as the objective function in kinematic designs. The objective function can be expressed as

$$\eta = \sqrt{\bar{\eta}^2 + (w_\eta \tilde{\eta})^2} \tag{31}$$

where $\tilde{\eta} = \max(\kappa)/\min(\kappa)$ with $\max(\kappa)$ and $\min(\kappa)$ representing the maximum and minimum values of $\kappa$ in the task workspace and $w_\eta$ representing the weight placed upon the ratio of $\bar{\eta}$ to $\tilde{\eta}$.

$\bar{\eta}$ and $\tilde{\eta}$ can be numerically calculated by

$$\bar{\eta} = \frac{1}{M \times N} \sum_{m=1}^{M} \sum_{n=1}^{N} \kappa_{mn}, \quad \tilde{\eta} = \frac{\max(\kappa_{mn})}{\min(\kappa_{mn})} \tag{32}$$

where $\kappa_{mn}$ is the value of $\kappa$ evaluated at node $(m, n)$ of $(M-1) \times (N-1)$ equally meshed $W_{\mathrm{t}}$.

# 5 Applications

## 5.1 XNZD2415 hybrid machine tool

A 2-DOF planar parallel manipulator was combined with a worktable having a translational DOF in the $z$ axis and a milling head with two rotational DOFs about the $x$ and $z$ axes to create a 5-DOF hybrid serial-parallel machine tool (XNZD2415). With the two-axis milling head, the tool can obtain any desired orientation in the task workspace, which provides high dexterity. The worktable can move freely along the $z$ axis, which enables the machine tool to manufacture long workpieces.

The task workspace $W_{\mathrm{t}}$ of the parallel manipulator is designed as a rectangle $b$=1600 mm in width and $h$= 1000 mm in height. The manipulator also has $\alpha_{\max} = 80^\circ$, $\beta_{\min} = 10^\circ$, and $r = 75$ mm. The singularity analysis shows that singularities cannot occur in the task workspace of the parallel manipulator.

The optimal design based on the task workspace results in $R = 1217.4$ mm. The other design parameters are then calculated by minimizing the objective function $\eta$. Figure 5 shows that $\eta$ has a minimum value of 1.916 when $l_1$=2060 mm for $w_\eta = 0.1$. Based on Eq. (26), it can be obtained that $|y_{i,\max} - y_{i,\min}|$ is 2345.2 mm.

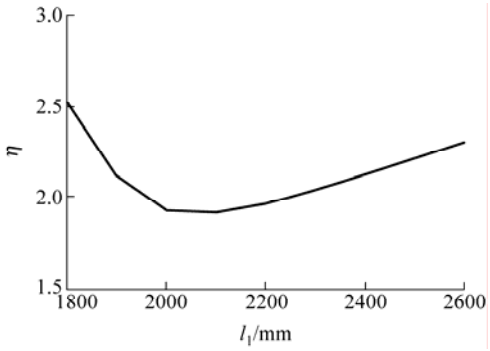


**Fig. 5 Minimization of $\eta$ for various link lengths**

The condition number of the Jacobian of the parallel manipulator in the machine tool is shown in Fig. 6. The distribution of the condition number is symmetrical about the $x$ axis. The good kinematic performance is achieved by balancing the conflict between $\bar{\eta}$ and $\tilde{\eta}$.

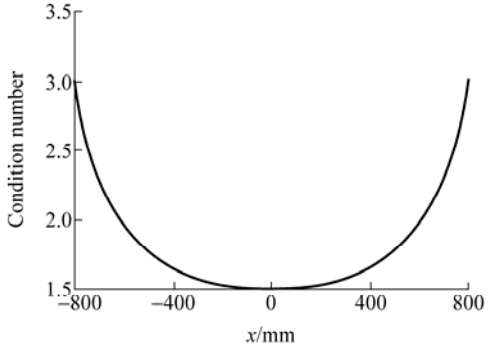


**Fig. 6 Condition number of the Jacobian of XNZD2415 machine tool**

The machine tool was built by Tsinghua University and was used in the Harbin Electric Machinery Co, Ltd in China to mill a series of blades and guide vanes for hydraulic turbine generator sets. The prototype is

shown in Fig. 7.


**Fig. 7 XNZD2415 hybrid machine tool**

### 5.2 XNZD2430 heavy duty machine tool

After the successful application of XNZD2415 for various machining tasks, Harbin Electric Machinery Co needed another hybrid machine tool to machine very large blades and guide vanes for hydraulic turbine generator sets.

Another heavy duty machine tool (XNZD2430) was then built based on the 2-DOF parallel manipulator. The new is similar to the first machine in structure with a much larger new workspace of XNZD2430 and some other modifications including two additional cover sheets fixed on the columns and an auxiliary tray fixed on top of the milling head. The sides of the cover sheets contact the auxiliary tray which is covered with copper sheet. The auxiliary tray contacts the two cover sheet and slides between them as the milling head moves. Therefore, the cover sheets limit the deformation of the milling head and improve the machine tool stiffness normal to the plane of the manipulator motion. Four brackets are also added to the new machine tool to improve the stiffness.

Two additional non-rotating milling heads were designed to replace the 2-DOF milling head for mounting on the side or underside of the moving platform. This heavy duty machine tool is then a 3-DOF machine which can machine vertically or horizontally.

The task workspace $W_t$ of the new parallel manipulator was designed as a rectangle $b$=3000 mm in width and $h$= 1800 mm in height with $\alpha_{\max} = 79^\circ$, $\beta_{\min} = 5^\circ$. The manipulator can not reach singular configurations in the task workspace.

The optimal design based on the task workspace results in $R = 2342.5$ mm. $\eta$ has a minimum value when $l_1$ =3550 mm and $w_\eta = 0.1$. $|y_{i,\max} - y_{i,\min}|$ can then be determined from Eq. (26). The main design parameters are listed in Table 1.

**Table 1 Results of optimization for XNZD2430 machine tool**

| Parameters | Values |
|---|---|
| $l_1$ | 3550 mm |
| $l_2$ | 3550 mm |
| $r$ | 550 mm |
| $\lvert y_{i,\max} - y_{i,\min} \rvert$ | 4010.7 mm |
| $\eta$ | 1.99 |

The distribution of $\kappa$ for the optimal design is shown in Fig. 8. The distribution shows that the condition number is also symmetrical with respect to the $x$ axis and the kinematic performance is optimal.

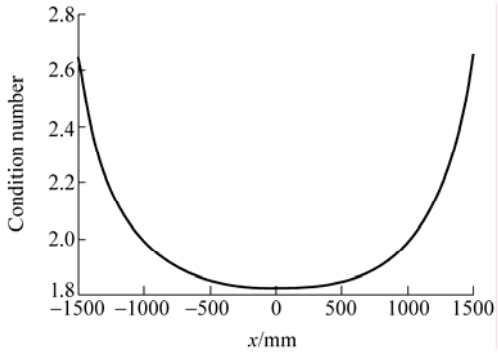


**Fig. 8 Condition number of the Jacobian of XNZD2430 machine tool**

The XNZD2430 machine tool shown in Fig. 9 is currently being built by Tsinghua University with the machine's dynamics and controls to be tested soon.

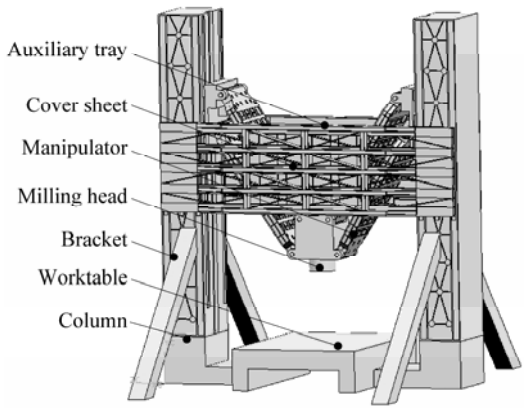


**Fig. 9 Prototype of XNZD2430 machine tool**

# 6 Conclusions

The kinematic design of a 2-DOF planar parallel manipulator has been investigated. The investigation is shown as follows.

(1) The distance between the two columns is determined by the optimum design based on the workspace.

(2) A global, comprehensive performance index, which includes both the mean and the range of the condition number of the Jacobian in the task workspace, can be used to effectively optimize the kinematic design.

(3) The planar parallel manipulator-based machine tool was successfully used to machine blades and guide vanes for a hydraulic turbine. Another heavy duty machine tool based on the parallel manipulator is being built for larger machining tasks.

## References


[1] Beqon P, Pierrot F, Dauchez P. Fuzzy sliding mode control of a fast parallel robot. In: IEEE International Conference on Robotics and Automation, 1995: 1178-1183.

[2] Ferraresi C, Pastorelli S, Sorli M, Zhmud N. Static and dynamic behavior of a high stiffness Stewart platform-based force/torque sensor. *Journal of Robotic Systems*, 1995, **12**(12): 883-893.

[3] Wu J, Li T M, Tang X Q. Robust trajectory tracking control of a planar parallel mechanism. *J. Tsinghua University* (*Sci. & Technol.*), 2005, **45**(5): 642-646. (in Chinese)

[4] Kock S, Schumacher W. Parallel *x-y* mechanism with actuation redundancy for high-speed and active-stiffness applications. In: IEEE International Conference on Robotics and Automation. Leuven. Belgium, 1998: 2295-2300.

[5] Liu X J, Wang Q M, Wang J S. Kinematics, dynamics and dimensional synthesis of a novel 2-DOF translational manipulator. *Journal of Intelligent and Robotic Systems*, 2004, **41**(4): 205-224.

[6] Wang J S, Tang X Q. Analysis and dimensional design of a novel hybrid machine tool. *International Journal of Machine Tools and Manufacture*, 2003, **43**(7): 647-655.

[7] Huang T, Li Z X, Li M, Chetwynd D G, Gosselin C M. Conceptual design and dimensional synthesis of a novel 2-DOF translational parallel robot for pick-and-place operations. *ASME Journal of Mechanical Design*, 2004, **126**(3): 449-455.

[8] Gao F, Liu X J, Gruver W A. Performance evaluation of two-degree-of freedom planar parallel robots. *Mechanism and Machine Theory*, 1998, **33**(6): 661-668.

[9] McCloy D. Some comparisons of serial-driven and parallel-driven manipulators. *Robotica*, 1990, **8**(4): 355-362.

[10] Arsenault M, Boudreau R. Synthesis of a general planar parallel manipulator with prismatic joints for optimal stiffness. In: The 11th World Congress in Mechanism and Machine Science. Beijing: China Machine Press, 2004: 1633-1637.

[11] Gosselin C M. Optimum design of robotic manipulators using dexterity indices. *Robotics and Autonomous Systems*, 1992, **9**(4): 213-226.

[12] Gosselin C M, Angeles J. A global performance index for the kinematic optimization of robotic manipulators. *ASME Journal of Mechanical Design*, 1991, **113**(3): 220-226.

[13] Huang T, Li M, Li Z X, Chetwynd D G, Whitehouse D J. Optimal kinematic design of 2-DOF parallel manipulators with well-shaped workspace bounded by a specified conditioning index. *IEEE Transactions on Robotics and Automation*, 2004, **20**(3): 538-543.

[14] Liu X J, Jin Z L, Gao F. Optimum design of a 3-DOF spherical parallel mechanisms with respect to the conditioning and stiffness indices. *Mechanism and Machine Theory*, 2000, **35**(9): 1257-1267.

[15] Gosselin C M, Angeles J. Singularity analysis of closed loop kinematic chains. *IEEE Transactions on Robotic and Automation*, 1990, **6**(3): 281-290.